Desalination 283 (2011) 214–220

Contents lists available at ScienceDirect

Desalination

journal homepage: www.elsevier.com/locate/desal

Effect of modified PVDF hollow fiber submerged ultrafiltration membrane for refinery wastewater treatment

E. Yuliwati [a,b], A.F. Ismail [a,b,*], T. Matsuura [a,c], M.A. Kassim [a], M.S. Abdullah [a]

[a] Advanced Membrane Technology Research Centre (AMTEC), Universiti Teknologi Malaysia, 81310 UTM, Skudai Johor, Malaysia
[b] Faculty of Petroleum and Renewable Energy Engineering, Universiti Teknologi Malaysia, 81310 UTM, Skudai Johor, Malaysia
[c] Department of Chemical Engineering, Industrial Membrane Research Laboratory, University of Ottawa, Ont., Canada KIN 6N5

ARTICLE INFO

Article history:
Received 1 January 2011
Received in revised form 16 March 2011
Accepted 17 March 2011
Available online 27 April 2011

Keywords:
PVDF membrane
Ultrafiltration
Surface hydrophilicity
Hollow fiber

ABSTRACT

Submerged ultrafiltration process was studied for treatment of refinery wastewater using PVDF hollow fiber membranes. The membranes were prepared via the phase inversion method by dispersing $LiCl \cdot H_2O$ and TiO_2 in the dope to study the effects of surface properties on membrane performance. The comparison of the performance and morphology was conducted on prepared PVDF composite membranes with various $LiCl \cdot H_2O$ and TiO_2 contents. The hollow fiber membranes were characterized by field emission scanning electron microscope (FESEM) and energy dispersive x-ray (EDX), average pore size and effective porosity measurements, contact angle measurement, permeability and rejection test. Maximum results were observed for membrane hydrophilicity, membrane porosity and average pore size when the TiO_2 concentration was 1.95%. It was also found that interactions between the membrane surface and suspended solid constituents strongly influenced the membrane fouling. The maximum flux and rejection of refinery wastewater were 82.5 L/m^2 h and 98.8%, respectively, when the PVDF composite membrane with TiO_2 content of 1.95% is used at pH = 6.9.

1. Introduction

A stringent environmental regulations and legislation have driven a great effort to seek alternative technologies for wastewater separation, which have the following important features: enhanced efficiency, self-sustainability, and absence of hazardous wastes. Several common techniques have been improved for removing soluble and insoluble of organic and inorganic contaminants from refinery wastewater, such as gravity settling separation and mechanical coalescence, coagulation and air flotation, electrostatic and electrocoagulation separation. However, these methods would lead to a huge production of sludge and complicated operation problems. Membrane technologies have enjoyed great popularity over the last 30 years and been extensively used in separation facilities to separate liquid/liquid or liquid/solid mixtures due to the flexibility and ability to remove the contaminant from wastewater to very low levels [1,2]. Moreover, because of its suitable pore sizes (usually in the range of 2–50 nm) and capability of removing emulsified oil droplets and other organic contaminant, ultrafiltration has been demonstrated as an efficient method in refinery wastewater treatment [3–5].

The ultrafiltration membrane is mainly classified into two kinds, namely, polymeric membranes and inorganic membranes. Due to the distinct advantages such as temperature and wear resistance, well-defined stable pore structure, and chemical inertness, the inorganic membranes such as, ceramic and carbon membranes are quite suitable for processes involving high temperatures and harsh chemical environments and have been successfully applied to the refinery wastewater treatment [6–8]. However, inorganic membranes display some inherent disadvantages and majority of them are related to their relatively high cost arising from the expensive materials, the complicated fabrication procedure and the low membrane surface [9]. Hence, the cheap and easy-fabricating polymeric membranes are still dominating the membrane market. It should be pointed out that the serious membrane fouling caused by nonspecific adsorption and/or deposition of the foulant onto the membrane surfaces, often results in a substantial decline of the permeate flux with operation time and consequently limits their wide application in the wastewater treatment [10]. Many investigations have demonstrated that modifying membrane surface, such as hydrophilicity, pore size, porosity and, surface charge effectively inhibited the nonspecific adsorption and consequently decreases membrane fouling and significantly increases the permeate flux [11–14].

Polyvinylidene fluoride (PVDF) is regarded as one of the most attractive polymer materials in microporous membrane industry. The molecular structure of PVDF homopolymer with alternating CH_2 and CF_2 groups along the polymer chain forms a unique polymer. It provides extraordinary mechanical properties, high chemical resistance, good thermal stability and excellent membrane forming abilities [15]. Therefore, PVDF is a suitable material to make membranes, which

* Corresponding author at: Advanced Membrane Technology Research Center (AMTEC), Universiti Teknologi Malaysia, 81310 UTM, Skudai Johor, Malaysia. Tel.: +60 7 553 5592; fax: +60 7 558 1463.
E-mail address: afauzi@utm.my (A.F. Ismail).

0011-9164/$ – see front matter © 2011 Elsevier B.V. All rights reserved.
doi:10.1016/j.desal.2011.03.049

have been applied in lithium ion batteries, pervaporation, wastewater treatment etc. They can also be used as composites with inorganic nanoparticles such as ZrO_2 [16], SiO_2 [17], TiO_2 [18,19], Al_2O_3 [20], and some small molecules salt such as LiCl [21] to improve the membrane separation performance, thermal ability, chemical stability, and membrane forming ability by the combination of the basic properties of organic and inorganic materials. Among different inorganic nanoparticles, TiO_2 has received the most attention because of its stability under harsh conditions, commercial availability, and easiness of preparation. When dispersed to PVDF membrane, TiO_2 nanoparticles can not only increase the hydrophilicity of membrane to enhance the flux but also kill bacteria and mitigate the fouling problem of PVDF membrane in MBR system [22,23].

The improvement of PVDF hollow fiber composite membrane properties could be achieved via sol-gel method, grafting, and physical blending of inorganic materials for its convenient operation [24]. Among these methods, physical blending is most interesting, owing to its convenient operation under mild conditions, and good performances of the resulting membranes [25,26]. Han et al. [27] reported that PVDF/SiO_2 and PVDF/TiO_2 composite hollow fiber membranes could result in better performance, especially in terms of membrane structure, mechanical strength, and permeation properties. Liu et al. [28] and Chiang et al. [29] have studied the preparation of TiO_2/Al_2O_3 composite hollow fiber membranes that exhibited better performances than the membranes with individually added TiO_2 or Al_2O_3 nanoparticles. At the present time, there are still few papers reporting the preparation and characterization of PVDF/multi-nanoparticle composite hollow fiber membranes, which might combine the advantages of polymer and various nanoparticles.

The effect of nanoparticle additives, i.e. LiCl and PVP, on the thermodynamic/kinetic relations during the phase inversion process in the preparation of PVDF-based membranes was investigated by Fontananova et al. [30]. These additives were soluble both in DMAc and H_2O, and were leached out of the solution during phase inversion process. The macrovoids became more accentuated and extended over the whole cross-section when PVP was present in the casting solution; on the contrary, a high LiCl concentration reduced macrovoid formation. The unique electronic, magnetic, and optical properties of nanoparticles improved the properties of polymer to a certain extent because of their small sizes, large surface areas, and strong activities [31–33]. The presence of finely dispersed inorganic particles in the polymer matrix has proven very useful in the improvement of membrane performance [34].

In this study, the modified PVDF hollow fiber composite membranes by addition of $LiCl \cdot H_2O$ and TiO_2 in various concentrations was investigated, in view of modifying membrane surface properties and improve the filtration performance. Hydrophilicity of membranes is usually expressed in terms of contact angle for a liquid drop on the membrane surface to measure the tendency for liquid to wet of the membrane surface. Measurement of the streaming potential is a method for determining the zeta potential of porous membranes in order to understand and control the charge-related phenomena. Pore size and porosity analysis of the PVDF hollow fiber composite membranes were investigated. The surface and inner structures, and elemental composition of the sample membranes were studied by FESEM and EDX. The performance for refinery wastewater treatment was characterized by pure water flux and rejection efficiency of refinery wastewater at various pH values of feed solution.

2. Experimental

2.1. Materials

Hollow fiber composite membranes were prepared using Kynar®740 PVDF polymer pellets purchased from Arkema Inc. Philadelphia, USA. DMAc (Synthesis Grade, Merck, >99%) was used as solvent without further purification. Lithium chloride monohydrate and titanium dioxide nanoparticles were used as inorganic additives. Both of them were purchased from Sigma-Aldrich and used as received. Glycerol was purchased from MERCK (Germany) and used as non-solvent or the post treatment of membrane. In all cases, tap water was used as the external coagulation bath medium in the spinning process.

2.2. Preparation of PVDF spinning dopes

Pre-dried (24 h oven dried at 50 °C) PVDF pellets were weighed and poured into pre-weighed DMAc solvent. The mixture was stirred to ensure thorough wetting of polymer pellets, prior to the addition of appropriate amounts of $LiCl \cdot H_2O$ at 50 °C. TiO_2 was then added to the mixture which was continuously stirred for 48 h (IKA-20-W) at 500 rpm until a homogenous solution was formed. The polymer solution was kept in a glass bottle and air bubbles formed in the dope were removed using water aspirator for several hours. The fully dissolved polymer solution was transferred to a stainless steel reservoir and left in the reservoir for 24 h at room temperature for degassing prior to spinning process. Solution viscosity was measured using rheometer (Bohlin Instrument Ltd.) at various temperatures between 25 and 50 °C.

2.3. Hollow fiber spinning

The hollow fiber spinning process by dry-jet wet phase inversion was described elsewhere [35]. The details of the spinning dope compositions and spinning parameters are listed in Tables 1 and 2.

Briefly, the polymer solution was pressurized through the spinneret at a controlled extrusion rate, while internal coagulant was adjusted at 1.4 mL/min. The hollow fiber that had emerged from the tip of the spinneret was guided through the two water baths at a take up velocity 13.7 cm/s, carefully adjusted to match free falling velocity, before landing in a final collection bath to complete the solidification process. The spun hollow fibers were immersed in the water bath for a period of 3 days, with daily change of the water, to remove the residual DMAc and the additives. Then, the hollow fibers were post-treated by leaving them in 10 wt.% glycerol aqueous solution for 1 day in order to minimize fiber shrinkage and pores collapse. After the fibers were dried for 3 days, they were ready for making hollow fiber test modules.

2.4. Membrane characterizations

Field emission scanning electron microscope (FESEM) (JEOL JSM-6700F) was used to examine the morphology of the spun PVDF hollow fiber composite membrane by standard methods. The membrane

Table 1
Spinning dope compositions.

Sample	PVDF wt.%	TiO_2 wt.%	$LiCl \cdot H_2O$ wt. %
PTL-0	19	0	0.98
PTL-5	19	1	0.98
PTL-10	19	1.95	0.98
PTL-15	19	2.85	0.98
PTL-20	19	3.8	0.98

Table 2
Spinning condition of PVDF hollow fiber membranes.

Dope extrusion rate (mL/min)	4.20
Bore fluid	H_2O
Bore fluid flow rate (mL/min)	1.40
External coagulant	Tap water
Air gap distance (cm)	1 cm
Spinneret o.d./i.d. (mm)	1.10/0.55
Coagulation temperature (°C)	25

samples were immersed in liquid nitrogen and fractured carefully. The samples were then dried in vacuum oven and coated with sputtering platinum before testing. The FESEM micrographs of cross-section and inner skin layer were taken at various magnifications. It produced photographs at the analytical working distance of 10 nm.

The static contact angle of membrane was measured by the sessile drop method using a DropMeter A-100 contact angle system (Maist Vision Inspection & Measurement Co. Ltd.) to characterize the membrane wetting behaviour. The hollow fibers were cut lengthwise and the deionized water droplets were deposited on the inner and outer membrane surfaces at 4 different points using a microsyringe respectively. A microscope with a long working distance 6.5× objectives was used to capture image. The average of measured values was taken as its water contact angle.

Asymmetric porous membranes were characterized by determination of porosity and average pore radius. The membrane porosity, ε, was defined as the volume of the pores divided by the total volume of the porous membrane. The membrane porosity was calculated using the following equation,

$$\varepsilon = \frac{\frac{(w_1 - w_2)}{\rho_W}}{\frac{(w_1 - w_2)}{\rho_W} + \frac{w_2}{\rho_P}} \times 100 \quad (1)$$

where ε is the porosity of the membrane (%), w_1 the weight of wet membrane (g), w_2 the weight of dry membrane (g), ρ_p the density of the polymer (g/cm^3) and ρ_w is the density of water (g/cm^3).

To prepare the wet and dry membranes, five spun hollow fibers with the length of 25 cm were selected after solvent was exchanged in tap water for 3 days. The fibers were immersed into the isopropanol for 3 days and distilled water for 3 days. The remaining water in the inner surface was removed using air flow, before weighing the membranes. The wet membranes were dried in vacuum oven for 12 h at 40 °C and weighted.

Average pore radius, r_m, was determined by filtration velocity method, in which pure water flux of the wet membrane was measured by applying pressure (0.1 MP) for a limited period (20 h). It represents the average pore size along the membrane thickness (↙) that was the difference between external radius and internal radius of the hollow fiber membrane. The test module containing 60 fibers with the length of 35 cm was used to determine water permeability. According to Guerout–Elford–Ferry equation, r_m could be calculated [36,37]:

$$r_m = \sqrt{\frac{(2.9 - 1.75\varepsilon) \times 8\eta \swarrow Q}{\varepsilon \times A \times \Delta P}} \quad (2)$$

where η is water viscosity (8.9×10^{-4} Pa s), ↕is the membrane thickness (m), ΔP is the operation pressure (0.1 MPa), ε is the porosity of the membrane (%), Q is volume of permeate water per unit time (m^3 s^{-1}), A is effective area of membrane (m^2).

The surface charge properties of modified PVDF membranes were determined by measuring the zeta potential. Zeta potential analysis of the membrane surface was conducted using SurPASS electrokinetic analyzer (DKSH-Anton Paar GmbH, Graz, Austria) to characterize the surface chemistry (acidic and basic functional groups). The sample inside the glass cylinder of the Cylinder Cell is mounted with its adapter on the dovetail guide at the SurPASS front side. The distance between the measuring head brackets of the cell holder was adjusted. The calibration of the pH electrode requires three buffer standard solutions of known pH values (e.g., pH 3, pH 7, and pH 10). The pH range was controlled by using HCl and NaOH solutions. The definition of the parameters for pressure and rinse programs with the SurPASS monitor is a step forward before the actual measurement. In order to define an appropriate pressure limit for the zeta potential determination, the target pressure should be entered for the pressure program and the maximum pressure for the rinse program. The proceeded data evaluation and measurement of zeta potential may define briefly.

2.5. Permeation flux and rejection of refinery wastewater measurements

The permeation flux and rejection of PVDF hollow fiber membranes were measured by submerged ultrafiltration experimental equipment at various pHs of the feed solution (4.0 to 9.7). The equipment is shown schematically in Fig. 1. An in-house assembled U-shape hollow fiber module, with a filtration area of 11.42 cm^2, was submerged in prepared suspension in a membrane reservoir with a volume of 14 L. A cross-flow stream was produced by air bubbling generated by a diffuser situated underneath the submerged membrane module for mechanical cleaning of the membrane module. The air bubbling flow rate per unit projection membrane area was set constantly to 1.8 L/min in order to maintain proper turbulence. The filtration pressure was supplied by a vacuum pump and controlled by a needle valve at 0.5 bar. The permeate flow rate was continually recorded using flow meter. The volume of the water permeation was determined by collecting the permeate sample in a graduated cylinder at specific time intervals.

The rejection test was carried out with synthetic refinery wastewater at various pH values (from 4.0 to 9.7). All experiments were conducted at 25 °C using a vacuum pump. Firstly, the pure water permeation flux (J_w) was measured at reduced pressure (0.5 bar) on the permeate side. Then, the permeation flux for the refinery wastewater (J_R) and rejection (R) were measured also at the reduced pressure on the permeate side.

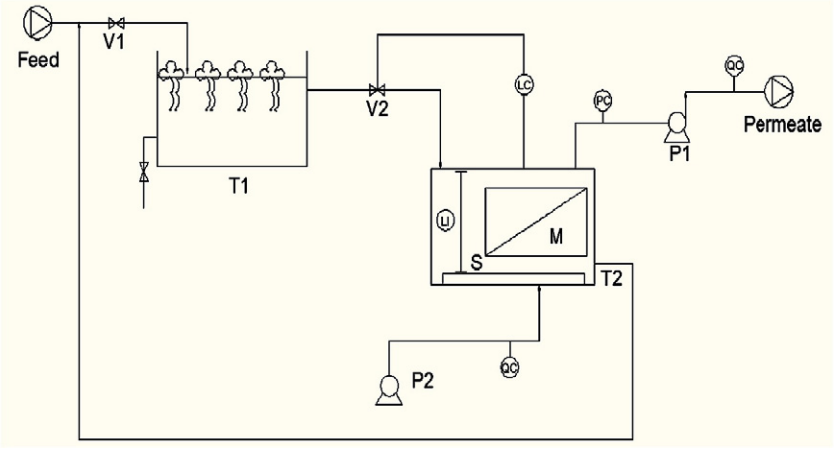

Fig. 1. Schematic of submerged ultrafiltration process: (v_1,v_2) feed flow, (P_1) peristaltic pump, (P_2) compressor, (S) sparger, (M) submerged membrane module, (T_1) pretreatment tank, (T_2) membrane reservoir, (QC) flow control, (PC) pressure control, (LC) level control, (LI) level indicator.

Membrane performance was tested with a self made U-shape membrane module having about 11.42 cm^2 of membrane surface area. Pure water permeation rate was measured after the steady state was reached, and the flux was calculated as

$$F = \frac{V}{At} \tag{4}$$

where F is the pure water flux (l/m^2 h), V is the permeate volume (l), A is the membrane surface area (m^2), and t is the time (h).

Rejection (R) was measured using the synthetic refinery wastewater after the pure water test. The synthetic refinery wastewater was in-house produced and consisted of fresh water, artificial seawater (ASTM D-1141-90): Standard Specification for Substitute Ocean Water [38], hydraulic oil, diesel fuel, surfactant, and carbon black in a proper composition, having mixed liquor suspended solid (MLSS) of 3 g/L and UV absorption at a wavelength of 254 nm (Perkin-Elmer Lamda 25 UV–vis spectrophotometer). The composition of synthetic refinery wastewater was shown in Table 3 and the rejection of refinery wastewater ultrafiltration was calculated as

$$R = \left(1 - \frac{c_p}{c_f}\right) \times 100 \tag{5}$$

where R is the rejection ultrafiltration process (%), c_p is the concentration of the permeate (%) and c_f is the concentration of the feed (%).

3. Results and discussions

3.1. Morphological studies of PVDF membranes

The PVDF hollow fiber membranes were fabricated using dry-jet wet spinning method with three different batches of fibers for each dope composition. The morphologies of the membrane were studied by FESEM.

Fig. 2 shows the FESEM micrographs of the PVDF hollow fiber composite membranes prepared using different concentrations of TiO_2 at a constant concentration of $LiCl \cdot H_2O$. Improvement of membrane morphology is observed for addition of a small amount of TiO_2 nanoparticles. TiO_2 nanoparticles have high specific areas and hydrophilicity, which will affect the mass transfer during the spinning process.

The cross-sectional images for all hollow fibers consist of finger-like macrovoids extending from both inner and outer walls of the hollow fiber, and an intermediate sponge-like layer. The thickness of the sponge-like layer decreases initially with an increase in TiO_2 concentration (from Fig. 3a to c). However, with a further increase in TiO_2 concentration the thickness of sponge-like layer starts to increase (Fig. 3d and e). This phenomenon can be explained by the kinetic effect on the rate of solvent-nonsolvent exchange in the phase inversion process. At lower TiO_2 concentration, an increase in the amount of hydrophilic TiO_2 tends to draw more water into the polymer dope, resulting in an increase in the length of finger-like macrovoids and decrease in the thickness of the intermediate sponge-like layer. Whereas at higher concentrations of TiO_2, an increase in TiO_2 concentration increases the viscosity of the polymer dope, decreasing the rate of water intrusion into the polymer dope, which results in the shorter finger-like macrovoids and thicker intermediate sponge-like layer.

Table 4 showed the EDX analysis of the modified PVDF membranes that was investigated to determine the experimental inorganic element composition. The result indicated the titanium, fluoride, lithium, chloride, oxide, and carbon elements and their existence in the membrane with a weight ratio of Ti:F:Li:Cl:O:C, as these inorganic elements were prepared by PTL-10, PTL-15, and PTL-20.

Table 3
The composition of refinery wastewater synthetic.

Constituent, unit	Influent	National primary discharged standard (P.U. (A) 434, Standard B, December 10, 2011)
pH	6.7	5.5–9.0
Oil and grease, mg/L	17.0	10.0
COD, mg/L	555.0	400.0
NH3-N, mg/L	29.1	20.0
Suspended solid, mg/L	213.0	100.0
Chlorine free, mg/L	4.6	2.0
Sulfide, mg/L	2.5	0.5

3.2. Porosity and hydrophilicity studies of PVDF membranes

Different concentrations of TiO_2 nanoparticles were employed to fabricate membranes. The membranes were characterized in terms of surface hydrophilicity (contact angle), average pore radius (r) and effective porosity (ε). The results are shown in Table 5.

Surface hydrophilicity is one of the most important properties of membranes which could affect the flux and antifouling ability of the membrane [39–41]. As presented in Table 5, the contact angle decreased significantly with increasing TiO_2 content up to 1.95 wt.% (PTL-10). The decreased contact angle indicates the increase in hydrophilicity, which seems natural considering high hydrophilicity of TiO_2 particles due to the presence of hydroxyl group. However, a further increase of TiO_2 concentration results in an increase in contact angle (decrease in hydrophilicity). This is most likely due to the agglomeration of TiO_2 nanoparticles, which reduces the area of contact of hydroxyl groups carried by the TiO_2 nanoparticles.

The porosity and average pore size of the prepared membranes are listed in Table 5. All the prepared membranes showed a good porosity in the range of 63 to 85%, which can be attributed to the low polymer concentration in the spinning dope and additives used. The porosity increased with an increase in TiO_2 content up to (PTL-10) but then decreased with further increase in TiO_2 content. This co insides with the change of the intermediate sponge layer thickness (initial decrease and then increase with further increase in TiO_2 content) as shown by the FESEM images.

The average pore radius is decreased with increasing TiO_2 concentration in the spinning dope due to the interaction between TiO_2, $LiCl \cdot H_2O$, and PVDF. A small proportion of TiO_2 nanoparticles in the dope obtained the existed interfacial stresses between the polymer and TiO_2 nanoparticles, which formed of the organic phase shrinkage during the demixing process. However, the added higher TiO_2 concentration blocked the pores and formed a denser cross-sectional substructure, consequently decreasing the average pore size. The change in the average pore size occurs parallel to the change in the porosity. This seems also natural considering the larger size of the finger-like pores as compared to the sponge-like pores.

3.3. Effect of surface properties on permeability and rejection

The effect of membrane characterization parameters on permeability and rejection was investigated using submerged UF experiments. As shown in Fig. 3, PTL-10 showed a maximum flux of 82.49 L/m^2 h for TiO_2 concentration of 1.95 wt.% (PTL-10). The rejection values demonstrated the similar trend to the flux, showing the maximum value of 98.8% at 1.95 wt.% TiO_2 concentration. It is interesting to note that the observed trend is contrary to the trade-off effect, by which rejection should decrease as flux increases. It is easy to understand that the flux shows a maximum value for the membrane PTL-10, since both porosity and pore size become the highest for this particular membrane (Table 5). The maximum in rejection occurring at the same TiO_2 concentration, on the other hand,

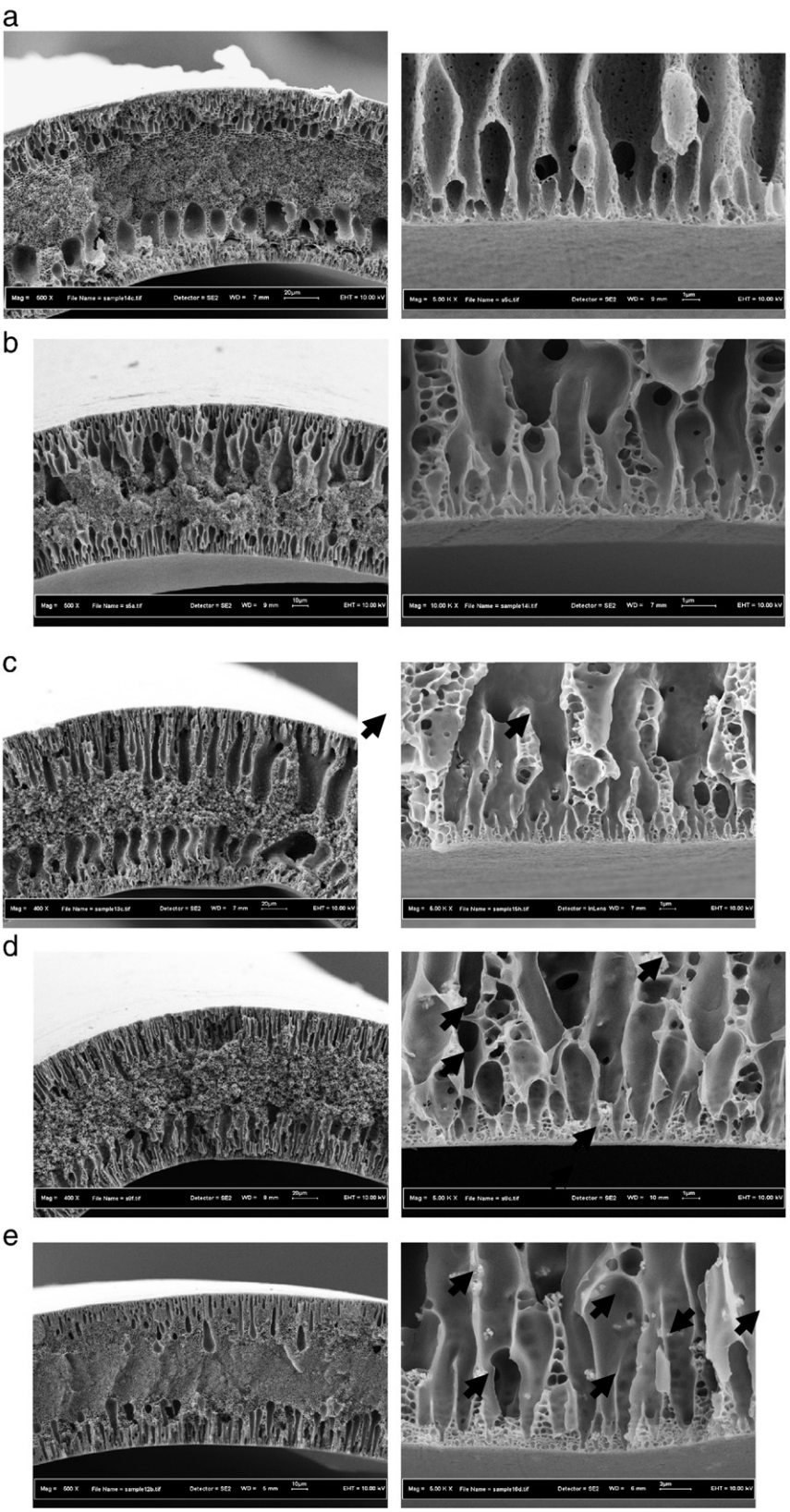

Fig. 2. The cross-sectional and outer surface images of hollow fibers (mag. 800×). (a) PTL-0 (b) PTL-5 (c) PTL-10 (d) PTL-15 (e) PTL-20.

can be explained by the trend observed in the surface hydrophilicity. As shown in Table 4, contact angle is the lowest, meaning hydrophilicity is the highest for PTL-10. Most likely, water is preferentially transported through the membrane as compared to the hydrophobic components of the refinery waste water when the membrane surface is hydrophilic, thus the highest rejection of oily components corresponds to the highest surface hydrophilicity of the membrane.

Table 4
The element composition of PVDF membranes top surface and cross-section.

Element, mass %	Membrane					
	PTL-10		PTL-15		PTL-20	
	Top surface	Cross-section	Top surface	Cross-section	Top surface	Cross-section
C	40.57	41.30	42.39	42.12	40.50	40.79
O	5.39	5.95	7.86	7.33	9.35	9.76
Ti	4.88	4.48	8.27	8.43	9.80	10.79
Cl	0.34	0.24	0.39	0.41	0.41	0.55
Li	0.23	0.20	0.24	0.22	0.23	0.20
F	25.90	25.95	25.50	26.48	25.29	25.87

Table 5
Properties of fabricated PVDF hollow fiber membranes.

Membrane	Contact angle (outer surfaces),° (s.d.)	Average pore size (nm), (s.d.)	Overall porosity (%)	Rejection (%)
PTL-0	81.05 (0.79)	28.0 (1.44)	66.96	62.56
PTL-5	60.90 (1.77)	14.93 (2.45)	76.96	82.35
PTL-10	47.33 (1.44)	34.05 (1.01)	85.41	98.83
PTL-15	56.63 (2.44)	30.12 (1.44)	74.67	93.90
PTL-20	57.67 (0.87)	26.07 (0.97)	63.26	91.71

TiO_2 particles on the membrane surface reduced the interaction between contaminants and the membrane surface. The increased membrane hydrophilicity and membrane pore size with lower TiO_2 concentration ($\leq$1.95 wt.%) could attract water molecules inside the composite membrane; facilitated their penetration through the membrane, enhancing the flux and rejection. However, higher TiO_2 concentration (>1.95 wt.%) resulted in the formation of a highly viscous dope. As a consequence, it decreased the hydrophilicity and average pore size. LiCl can be associated to the formation of a complex with DMAc, and able to have a network with an electron donor group of PVDF. A PVDF complex structure on the surface is the amorphous polymer chain physically cross-linked by the dissociated Li^+ and Cl^- ions through coordination with polymer and TiO_2 nanoparticles. The Li^+ could have direct coordination with F atom in PVDF matrix in the salt complex [29]. Li^+, Cl^-, F^- in PVDF chain, O^- in TiO_2 are Lewis bases as they have free electron. Li^+ behave as Lewis acids. When Li^+ is close to O^- of TiO_2, then titanium moves in the opposite direction due to coulomb attraction and cross-links with the base character of fluorine atom in PVDF [14,21]. Good affinity between LiCl and water makes also the water easily penetrate into the nascent membrane. The permeation flux increases and rejection decreases with adding LiCl in the spinning dope. It was also evidenced with EDX spectra which Li^+ is apparent in PVDF/LiCl/TiO_2 membrane as shown in the revised manuscript Table 3.

The antifouling properties of PVDF ultrafiltration membranes can be evaluated by the ratio of refinery wastewater flux (J_R) and pure water flux (J_W). For the higher antifouling submerged UF membrane, the feed of refinery wastewater would cause a smaller flux loss and the ratio (J_R/J_W) would become higher. Fig. 3 also shows that the ratio (J_R/J_W) first increased and reached the maximum at TiO_2 concentration of 1.95 wt.%. This is also due to the highest hydrophilicity at this particular TiO_2 concentration, science high hydrophilicity reduces the interaction between the hydrophobic contaminants and the membrane surface, effectively improving the antifouling properties. This clearly demonstrates the antifouling properties of TiO_2 when it is added to PVDF ultrafiltration membranes.

3.4. Effect of pH on flux performances

The flux is also strongly influenced by the pH value of feed solution. The permeate flux of a PVDF composite membrane (PTL-10) at various pH values of 4.0, 5.0, 6.9, 8.1 and 9.7 during refinery wastewater treatment is presented in Fig. 4. The steady flux increased sharply with increasing pH from 4.0 to 6.9 and the increase became less steep from pH 6.9 to 9.7 due to the chemical interactions between the charged membrane surface and oil droplets. Fig. 4 also shows the effect of pH on the zeta potential. The modified PVDF membrane (PTL-10) showed positive zeta potential in the values 59, 63, 71, 74, and 78 mV for pH range from 4.0 to 9.7. The positive zeta potential of the modified membranes is due to the dispersion of TiO_2 in the dope solution. Moreover, due to the presence of the surfactant (sodium dodecylallyl sulfosuccinate), the oil droplet is negatively charged. Therefore, the electrostatic affinity accelerates fouling formation since the droplets adsorb onto the membrane surface and penetrate into the membrane pores, lowering the steady permeate flux at pH 4.0. Thus, at lower pH values, the increase in suspended solid aggregation, and in turn flux reduction caused by formation of a thicker suspended solid deposit, is likely due to reduction of electrostatic repulsion.

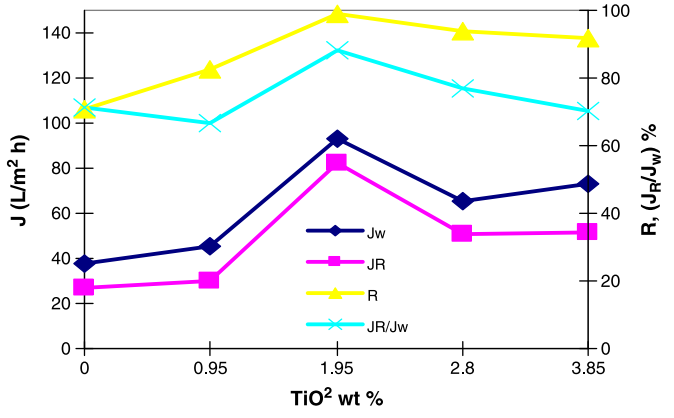

Fig. 3. J_w, J_R, R (retention), and the ratio J_R/J_w of PVDF/LiCl/TiO_2 composite membranes as a function of TiO_2 concentration.

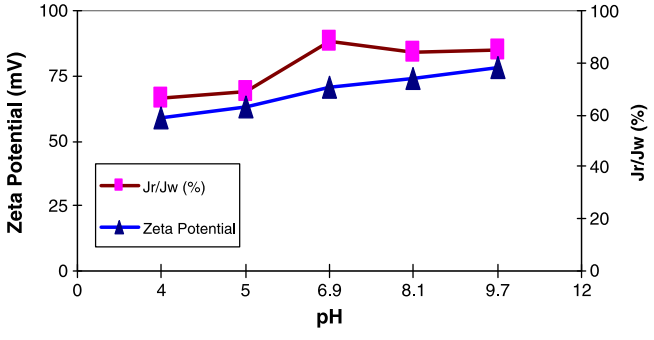

Fig. 4. Effect of solution pH and zeta potential on the steady flux during filtration of refinery wastewater (MLSS 3 g/L) by membrane PTL-10.

Repulsive forces reduce the adsorption of the foulant and limit the membrane pore blocking, which increases the permeability and results in higher permeate flux. As discussed by Yuan and Zydney [42], the initial flux decline during membrane filtration is due to the physical deposition of large suspended solid aggregates on the membrane surface. It was reported that lower pH induced a lower flux. Additionally, the slightly flux decline seen from pH 6.9 to 9.7 was caused by foulant deposition on the upper surface of the membrane at higher pH. Briefly, the flux is higher at higher pH values.

4. Conclusions

PVDF composite hollow fiber membranes were prepared using dry-jet wet spinning process. Various amounts of TiO_2 at a constant value of $LiCl \cdot H_2O$ were used as non-solvent additives in the spinning dopes to improve the phase-inversion rate and provide porous asymmetric membranes with improved structure for refinery produced wastewater treatment. Various characterizations and measurement techniques such as membrane structure, surface wettability, porosity, average pore size, and permeability were utilized to evaluate fine structural details of the membrane and membrane performance. Refinery produced wastewater filtration was conducted through prepared PVDF composite hollow fiber membranes. FESEM analysis indicated that PVDF concentration of 19 wt.% had suppressed both inner and outer membrane surface finger-like macrovoids with slightly denser skin layer which decreased mass transport resistance. Addition of 1.95 wt.% of TiO_2 nanoparticles resulted in smaller nanoparticles which in turn achieved higher hydrophilicity, small pore size, and high porosity. Permeability test illustrated that $LiCl \cdot H_2O$ and TiO_2 nanoparticles affected the PVDF membranes performance remarkably. Significantly higher flux and rejection of refinery wastewater were observed. Furthermore, the steady permeate flux achieved the decreased results at pH 6.7 to 9.7 slightly. These values also reflected the obtained thicker suspended solid deposit on the membrane outer surface. Briefly higher steady flux can be obtained at higher pH of feed solution.

References

[1] J.F. Kong, K. Li, Oil removal from oil-in-water emulsions using PVDF membranes, J. Membr. Sci. 16 (1999) 83–93.
[2] S.P. Deshmukh, K. Li, Effect of ethanol composition in water coagulation bath on morphology of PVDF hollow fibre membranes, J. Membr. Sci. 150 (1998) 75–85.
[3] A.F. Ismail, M.I. Mustaffar, R.M. Illias, M.S. Abdullah, Effect of dope extrusion rate on morphology and performance of hollow fiber membranes for ultrafiltration, Sep. Purif. Technol. 49 (2006) 10–19.
[4] A.F. Viero, T.M. Melo, A.P.R. Torres, N.R. Ferreira, G.L. Sant'Anna Jr., C.P. Borges, V.M.J. Santiago, The effects of long-term feeding of high organic loading in a submerged membrane reactor treating oil refinery wastewater, J. Membr. Sci. 319 (2008) 223–230.
[5] L.E. Fratila-Apachitei, M.D. Kennedy, J.D. Linton, I. Blume, J.C. Schippers, Influence of membrane morphology on the flux decline during dead-end ultrafiltration of refinery and petrochemical wastewater, J. Membr. Sci. 182 (2001) 151–159.
[6] F.L. Hua, Y.F. Tsang, Y.J. Wang, S.Y. Chan, H. Chua, S.N. Sin, Performance study of ceramic microfiltration membrane for oily wastewater treatment, Chem. Eng. J. 128 (2007) 169–175.
[7] S. Koonaphapdeelert, K. Li, Preparation and characterization of hydrophobic ceramic hollow fiber membrane, J. Membr. Sci. 291 (2002) 399–415.
[8] Y.S. Li, L. Yan, C.B. Xiang, L.J. Hong, Treatment of oily wastewater by organic–inorganic composite tubular ultrafiltration (UF) membranes, Desalination 196 (2006) 76–83.
[9] J. Saien, H. Nejati, Enhanced photocatalytic degradation of pollutants in petroleum refinery wastewater under mild conditions, J. Hazard. Mat. 148 (2007) 491–495.
[10] M.L. Hami, M.A. Al-Hashimi, M.M. Al-Doori, Effect of activated carbon on BOD and COD removal in a dissolved air flotation unit treating refinery wastewater, Desalination 216 (2007) 116–122.
[11] Q. Li, Z.L. Xu, L.Y. Yu, Effect of mixed solvents and PVDF types on performances of PVDF microporous membranes, J. Appl. Polym. Sci. 115 (2010) 2277–2287.
[12] N.A. Ochoa, M. Masuelli, J. Marchese, Effect of hydrophilicity on fouling of an emulsified oil wastewater with PVDF/PMMA membranes, J. Membr. Sci. 226 (2003) 203–211.
[13] T.H. Bae, I.C. Kim, T.M. Tak, Preparation and characterization of fouling-resistant TiO_2 self-assembled nanocomposite membrane, J. Membr. Sci. 275 (2006) 1–5.
[14] A. Bottino, G. Capanelli, S. Munari, A. Turturro, High performance ultrafiltration membranes cast from LiCl doped solution, Desalination 68 (1998) 167–177.
[15] M. Khayet, T. Matsuura, Preparation and characterization of polyvinylidene fluoride membranes for membrane distillation, Ind. Eng. Chem. Res. 40 (2001) 5710–5718.
[16] A.F. Ismail, T.D. Kusworo, A. Mustafa, Enhanced gas permeation performance of polyethersulfone mixed matrix hollow fiber membranes using novel Dynasylan Ameo Silane agent, J. Membr. Sci. 319 (1–2) (2008) 306–312.
[17] S. Chabot, C. Roy, G. Chowdhury, T. Matsuura, Development of poly(vinylidene fluoride) hollow fiber membranes for the treatment of water/organic vapor mixtures, J. Appl. Polym. Sci. 65 (1997) 1263–1270.
[18] X. Cao, J. Ma, X. Shi, Z. Ren, Effect of TiO_2 nanoparticle size on the performance of PVDF membrane, Appl. Surf. Sci. 253 (2006) 2003–2010.
[19] Y.J. Wang, D.J. Kim, Crystallinity, morphology, mechanical properties and conductivity study of in situ formed PVDF/$LiClO_4$/TiO_2 nanocomposite polymer electrolytes, Electrochim. Acta 52 (2007) 3181–3189.
[20] Y.S. Li, L. Yan, C.B. Xiang, L.J. Hong, Treatment of oily wastewater by organic–inorganic composite tubular ultrafiltration (UF) membranes, Desalination 196 (2006) 76–83.
[21] A. Mansourizadeh, A.F. Ismail, Effect of LiCl concentration in the polymer dope on the structure and performance of hydrophobic PVDF hollow fiber membranes for CO_2 absorption, Chem. Eng. J. 165 (3) (2010) 980–988.
[22] A.W. Zularisam, A.F. Ismail, R. Salim, Sakinah Mimi, H. Ozaki, The effects of natural organic matter (NOM) fractions on fouling characteristics and flux recovery of ultrafiltration membranes, Desalination 212 (1–3) (2007) 191–208.
[23] A.W. Zularisam, A.F. Ismail, R. Salim, Behaviour of natural organic matter in membrane filtration for surface water treatment: a-review, Desalination 194 (2006) 211–231.
[24] M. Khayet, C.Y. Feng, K.C. Khulbe, T. Matsuura, Preparation and characterization of polyvinylidene fluoride hollow fiber membranes for ultrafiltration, Polymer 43 (2002) 3879–3890.
[25] C.S. Feng, B.I. Shi, G.M. Li, V.I. Wu, Preparation and properties of microporous membrane from poly(vinylidene fluoride-co-tetrafluoroethylene) for membrane distillation, J. Membr. Sci. 237 (2004) 15–24.
[26] E. Yuliwati, A.F. Ismail, Effect of additives concentration on the surface properties and performance of PVDF ultrafiltration membranes for refinery wastewater treatment, Desalination 273 (1) (2011) 226–234.
[27] L.F. Han, Z.L. Xu, L.Y. Yu, Y.M. Wei, Y. Cao, Performance of PVDF/multi-nanoparticles composite hollow fiber ultrafiltration membranes, Iran. Polym. J. 19 (7) (2010) 553–565.
[28] Y. Liu, M.L. Yeow, K. Li, Preparation of porous PVDF hollow fibre membrane via a phase inversion method using lithium perchlorate ($LiClO_4$) as an additive, J. Membr. Sci. 258 (2005) 16–22.
[29] C.Y. Chiang, M.J. Reddy, P.P. Chu, Nano-tube composite PVDF/$LiPF_6$ solid membranes, Solid State Ionics 175 (2004) 631–635.
[30] E. Fontananova, J.C. Jansen, A. Cristiano, E. Curcio, E. Drioli, Effect of additives in the casting solution on the formation of PVDF membranes, Desalination 192 (2006) 190–197.
[31] Y. Yang, H. Zhang, P. Wang, Q.Z. Zheng, J. Li, The influence of nano-sized TiO_2 fillers on the morphologies and properties of PSF UF membrane, J. Membr. Sci. 288 (2007) 231–238.
[32] S.J. Oh, N. Kim, Y.T. Lee, Preparation and characterization of PVDF/TiO_2 organic–inorganic composite membranes for fouling resistance improvement, J. Membr. Sci. 345 (2009) 13–20.
[33] D. Wang, K. Li, W.K. Teo, Porous PVDF asymmetric hollow fiber membranes prepared with the use small molecular additives, J. Membr. Sci. 178 (2000) 13–23.
[34] J.P.G. Villaluenga, M. Khayet, M.A. López Manchado, J.L. Valentin, B. Seoane, J.I. Mengual, Gas transport properties of polypropylene/clay composite membranes, Eur. Polym. J. 43 (2007) 1132–1143.
[35] M. Khayet, C.Y. Feng, K.C. Khulbe, T. Matsuura, Study on the effect of a non-solvent additive on the morphology and performance of ultrafiltration hollow fibre membranes, Desalination 148 (2002) 321–327.
[36] L.Y. Yu, H.M. Shen, Z.L. Xu, PVDF-TiO_2 composite hollow fiber ultrafiltration membranes prepared by TiO_2 sol-gel method and blending method, J. Appl. Polym. Sci. 113 (2009) 1763–1772.
[37] G. Wu, S. Gan, L.Z. Cui, Y.Y. Xu, Preparation and characterization of PES/TiO_2 composite membranes, Appl. Sur. Sci. 254 (2008) 7080–7086.
[38] H. Peng, A.Y. Tremblay, The selective removal of oil from wastewaters while minimizing concentrate production using a membrane cascade, Desalination 229 (2008) 318–330.
[39] C.H. Lu, W.H. Wu, R.B. Kale, Microemulsion-mediated hydrothermal synthesis of photocatalytic TiO_2 powders, J. Hazard. Mat. 154 (2008) 649–654.
[40] S.H. Kim, S.Y. Kwak, B.H. Sohn, T.H. Park, Design of TiO_2 nanoparticles self-assembled aromatic polyamide thin-film-composition (TFC) membranes as approach to solve biofouling problem, J. Membr. Sci. 211 (2003) 157–165.
[41] S.J. Oh, N. Kim, Y.T. Lee, Preparation and characterization of PVDF/TiO_2 organic–inorganic composite membranes for fouling resistance improvement, J. Membr. Sci. 345 (2009) 13–20.
[42] W. Yuan, A.L. Zydney, Humic acid fouling during ultrafiltration, Environ. Sci. Technol. 34 (23) (2000) 5043–5050.